J. Fluid Mech. (1976), *vol.* 73, *part* 3, *pp.* 565–591
Printed in Great Britain

Turbulent flow past a porous plate

By J. M. R. GRAHAM
Department of Aeronautics, Imperial College, London

(Received 28 November 1973 and in revised form 18 September 1975)

The method of Vickery for calculating the drag of plane lattice structures normal to a turbulent stream is extended to cases of increased solidity. The analysis incorporates an extended version of Taylor's theory for the flow through a porous plate, and a simplified version of Hunt's analysis of the distortion of a turbulent flow by the mean flow field of a body. Some comparisons are made with experimental data.

1. Introduction

The main methods of calculating the unsteady wind loads on a structure in turbulent flow make use of quasi-steady theories such as those of Davenport (1961) and Vickery (1965), in which the body is assumed to react to the turbulent flow as it would to small slow changes in mean flow, with perhaps some appropriate alteration of the force coefficients. These theories lead to a linear relationship between unsteady loading and the relevant free-stream component of fluctuating velocity.

Hunt (1972) pointed to limitations in the use of these theories, particularly in cases in which the body size is comparable with the scale of the turbulence, as often occurs in practice. The quasi-steady method fails on two counts. First, no account is taken of the potential flow field, whose normal velocity component cancels the normal velocity component of the incident turbulence over the surface of the body. Treatment of this effect has largely been limited to the analysis of wings and aerofoils in turbulence. Second, no account is taken of the distortion of the turbulence by the interaction of the mean flow field of the body with the turbulent vorticity. Lighthill (1956) considered these two effects. He listed them in terms of three velocity fields induced by a body placed in a rotational stream: (i) a gradient of potential whose normal velocity component on the body surface cancels that of the primary flow; (ii) a Biot–Savart velocity field resulting from the change in vorticity in the primary flow; (iii) a gradient of potential the same as (i), but cancelling (ii) on the surface. Clearly, if (ii) can be calculated and added to the primary flow, (i) and (iii) can be calculated as a single potential field. This is the approach of Hunt (1973).

Hunt (1973) showed that rapid-distortion theory (Batchelor & Proudman 1954; Ribner & Tucker 1952) is particularly applicable to the analysis of external turbulent flows round bodies. He extended the theory to analyse, as an example, the problem of a turbulent cross-flow past a circular cylinder and calculated certain asymptotic and other special cases, notably the behaviour of the turbulence along the stagnation streamline. Some of the main predictions of the theory, which was the first full application of rapid-distortion theory to external flows,

have been corroborated by the experiments of Bearman (1971) and Petty (1970, private communication). But it was not possible to calculate general results, partly because the nonlinear effect of the mean velocity on the turbulence led to multiple numerical integrations.

In some cases, as in this paper, this difficulty can be avoided when it is possible to linearize these terms and still calculate the distortion effect to a reasonable degree of accuracy. The porous plate is such a case, because the mean-velocity perturbation is everywhere small, so that this linearization is possible.

The porous plate case is also worth analysing, because of its relevance both to Vickery's (1965) theory and to the problem of a solid plate normal to a turbulent flow, which has been extensively studied experimentally. Vickery (1965) analysed a rectangular plane lattice structure placed normal to the incident stream. He assumed that the turbulent velocities were much smaller than the mean velocity, and that the lattice was sufficiently tenuous for its back reaction on the incident flow to be considered negligible. With these assumptions, the theory related the local loading linearly to the undisturbed streamwise component of turbulent velocity 'incident' on the same point, and hence the drag spectrum to a double area integral of these velocity components. Bearman (1969) simplified this formula for the drag to one double integral of the appropriate cross-spectrum, and Roberts (1971) generalized the analysis to different shapes and spectra. Both Vickery and Bearman, in these papers, compared their calculated values of aerodynamic admittance of drag predicted by the theory with measurements made on solid plates normal to a turbulent airstream behind a wind tunnel grid. A solid plate is obviously a severe test of the second of Vickery's assumptions; nevertheless, the predicted and observed values were comparable, although important discrepancies appeared. The first assumption, limiting the turbulence intensity, is the less restrictive, since it is reasonably well satisfied in many cases of both the atmosphere and the wind tunnel. In the present paper, the importance of the second assumption is examined by constructing a higher-order approximation to the theory in terms of the porosity of the structure.

Vickery's idealized plane lattice is a structure whose separate members are of sufficiently small width, compared with any other non-viscous length scale, to have negligible individual effect on the flow, but which together effectively form a uniform sheet of resistance to the flow. This structure is the same in principle as Taylor's model for a porous plate (1944) and the representations of wire gauzes investigated by many authors.

The main effect of such a structure is to produce a drop in the total pressure along any streamline passing through it. Schubauer, Spangenberg & Klebanoff (1950) suggested the formula for a gauze

$$\Delta p = \tfrac{1}{2}K(\theta_1)\rho q^2.$$

Δp is the pressure drop, ρ the fluid density, K the resistance coefficient of the gauze, a function of the local inlet flow angle θ_1 (see figure 1), and q is the local flow speed through the gauze. The gauze also refracts the streamlines, and the formula for the outlet flow angle $\theta_2 = \alpha\theta_1$ was suggested. (α is the refractive index of the gauze, and may depend on θ_1.)

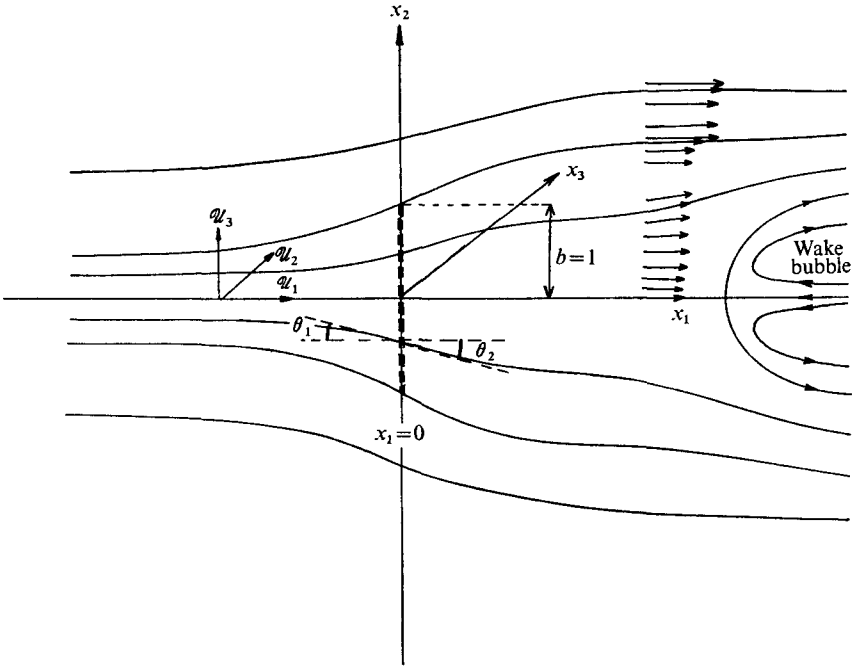

FIGURE 1. Plate and axes.

Subsequently various formulae were proposed, to describe the dependence of K and α on θ_1 and the geometry of the gauze. In the limit of a very porous plate or gauze and weak turbulence, they all lead to similar results, which are compatible with Vickery's analysis.

Schubauer's formulae were used by Taylor & Batchelor (1949) to calculate the effect of a homogeneous gauze of infinite extent on a turbulent flow passing through it normally. Their analysis was linearized, using the relative turbulence intensity as the small parameter, and was valid for all values of K and α. This was possible because the gauze, being of infinite extent, did not perturb the mean flow. In addition, because of the assumed low intensity of the turbulence, $K(\theta_1)$ and $\alpha(\theta_1)$ were approximated by their values at $\theta_1 = 0$: $K(0)$, hereafter referred to as K, and $\alpha(0)$, hereafter α. But this analysis is not applicable to gauzes of finite extent, because of the effects of distortion of the turbulence by the mean-velocity field and the more complicated boundary conditions.

Analyses of *mean* flows through gauzes and porous plates include the cases of oblique and non-homogeneous gauzes (investigated by e.g. Elder 1959; Lau & Baines 1968; Turner 1969; Owen & Zienkiewicz 1957) and Taylor's (1944) investigation of the porous plate. Taylor (1944) approaches the problem directly, by representing the plate as a source density distribution m for which $\Delta p = \rho \overline{U} m$, where the pressure jump across the plate along a normal Δp is also related to the normal velocity component at the plate $\overline{U}$ by $\Delta p = \frac{1}{2} K \rho \overline{U}^2$.

This is the same as the general gauze formula above, with $\alpha = 1$ everywhere (i.e. no refraction), and $K(\theta_1) = K \cos\theta_1$. The predictions of drag coefficient C_D given by Taylor were compared with experimental values by Taylor & Davies

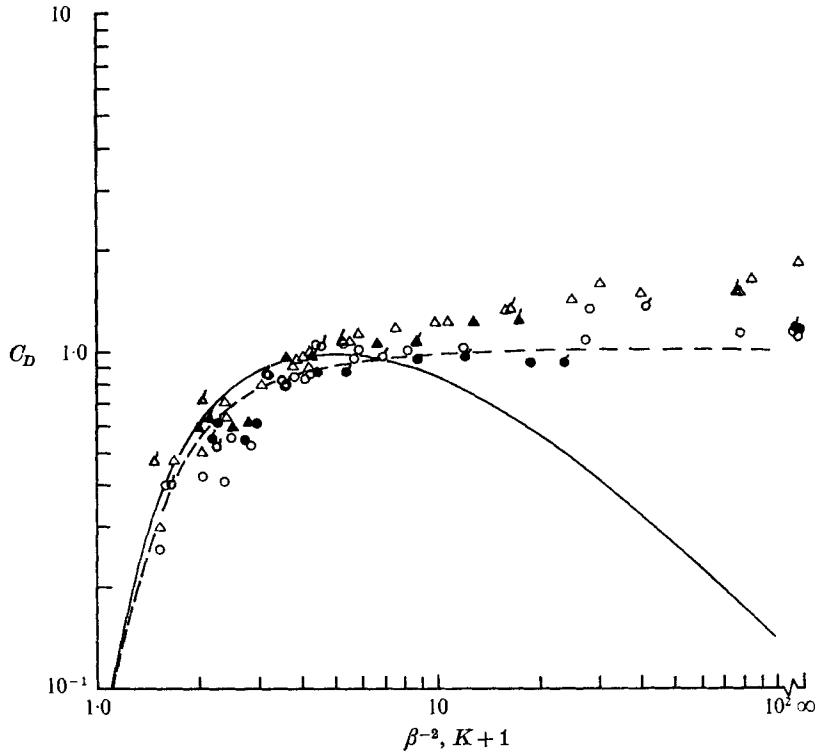

FIGURE 2. Drag coefficients of porous plates. C_D: ——, Taylor; – – –, Koo & James. Two-dimensional plates: △, Castro, Blockley, Valensi, Rebont; ▲, this experiment. Three-dimensional plates: ○, Taylor & Davies, DeBray; ●, this experiment. A flag indicates C_D plotted against K rather than β.

(1944) and Blockley (1968). Their results, and those of Valensi & Rebont (1969), Castro (1971) and DeBray (1957), are summarized in figure 2. There is a difficulty in comparing some of the results with Taylor's theory, since in many cases the plate is designated by its open-area ratio β, and the resistance coefficient K has not been measured. But, as far as comparison is possible, the Taylor drag coefficient

$$C_D = K/(1+\tfrac{1}{4}K)^2$$

is in reasonable agreement with most of the experimental values up to a value of the porosity at which Castro found that the recirculating 'bubble' region in the wake had moved forward into the vicinity of the plate. Above this value of K (about 4), the theoretical drag coefficient is too low, and both Castro, for two-dimensional plates, and DeBray, for square ones, found that a 'vortex shedding' peak started to appear in the velocity spectrum of the wake. Koo & James (1973) proposed a rather better theory, which gives values of drag coefficient close to those given by Taylor for $K \leqslant 4$, and a more realistic, monotonically increasing, drag coefficient at higher values of K. However, the Taylor theory does have the advantage of leading to simple equations, and for this reason a resistance equation based on it has been adopted here. The values of mean drag coefficient given by Taylor's theory for $K > 4$ are unrealistic, and

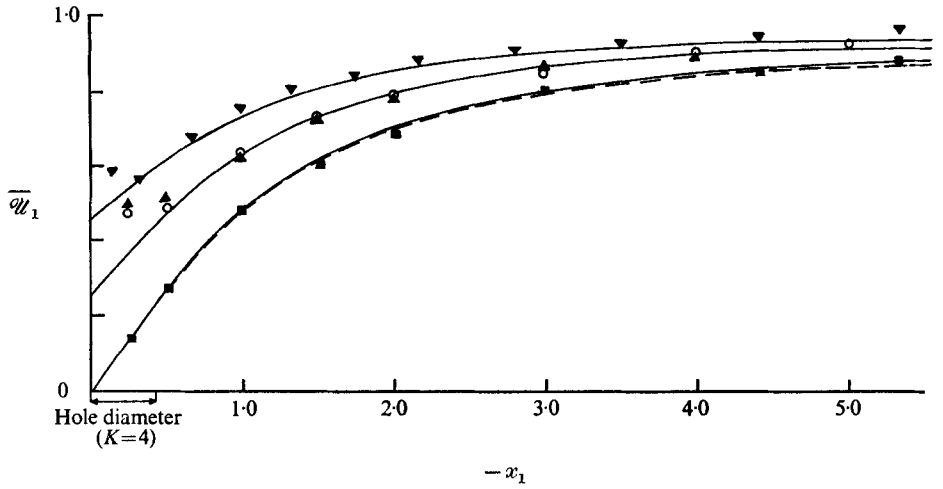

FIGURE 3. Mean velocity along upstream centre-line. Measured K: ▼, 4·5; ▲, 11; ■, ∞; ○, 11, larger-scale turbulence. Calculated: ——, Taylor; – – –, Parkinson & Jandali ($C_{pb} = -1{\cdot}08$).

for that reason the prediction of unsteady drag forces by this method has been limited to $K \leqslant 4$. But the mean-velocity field in the neighbourhood of the plate is quite well represented by the theory, for all values of K, even up to the solid plate ($K = \infty$). Values of centre-line velocity are compared with measured data and with values given by the source-wake method of Parkinson & Jandali (1970) in figure 3.

A further limitation on the magnitude of K is required by the linearized analysis for distortion of the turbulence by the mean-velocity field of the plate. This linearization is only reasonable if the mean-velocity perturbation is small over most of the region that affects the distorted turbulent velocity field. Since Taylor's theory predicts the mean flow quite accurately far from the plate where the perturbation is small for all K, the present method should predict the distorted turbulent velocity field accurately far from the plate. But the turbulence close to the plate, and hence also its unsteady drag, will only be predicted accurately for K small enough that the mean-velocity perturbation is small there also.

If the plate is regarded as a gauze, the simplified equations for the pressure drop and refraction are equivalent to the more general equations when K is small compared with one. But assuming that Taylor's theory describes the mean flow field of the plate reasonably accurately for $K \leqslant 4$, the present analysis, being a time-dependent extension of it, linearized with respect to the mean-velocity perturbation of order $K/(4+K)$, is a good approximation when K is small compared with 4. Therefore, the term 'small', when applied to K, will be used here to mean 'small compared with 4'. In fact Taylor's theory breaks down for all K at the edges of the plate, where the spanwise velocity is predicted to have a weak logarithmic singularity. This is unrepresentative of the real flow, but appears to have negligible effect on the calculated turbulence, except very close to the edges.

Since the resistance equation is based on Taylor's theory, the structure will be referred to hereafter as a porous plate, rather than a lattice or a gauze. Further, we shall assume, as have all similar flow analyses, that the effect of Reynolds number is small, and is confined to the value of the parameter K, so that K may be taken as a constant for any particular case of mean flow speed and hole geometry, but that in this respect the extent of the plate is immaterial.

2. Analysis

2.1. *Linearization of the vorticity transport equation*

We suppose that the free stream has mean velocity $\overline{U}_\infty$ normal to a two-dimensional porous plate of width $2b$, as in figure 1. The mean flow convects from far upstream homogeneous, isotropic turbulence, with velocity components $u_{i\infty}$ in the directions x_i (1 streamwise, 2 across, 3 spanwise). $\overline{u}_{i\infty} = 0$, where the overbar denotes a time mean and the turbulence is weak, i.e.

$$\overline{u}_{1\infty}^{2\frac{1}{2}}/\overline{U}_\infty = O(\epsilon) \ll 1.$$

Introducing the porous plate into the flow at $x_1 = 0$ generates disturbance velocities $\bar{\mathbf{u}}_0$ (mean) + $\mathbf{u}$ (fluctuating). $\bar{\mathbf{u}}_0$ can be divided into two parts: $\bar{\mathbf{u}}$, the mean perturbation which would occur in the absence of turbulence and which is $O(K\overline{U}_\infty)$ for small K, and $\bar{\mathbf{u}}'$, a component arising from cross-coupling between the effects of the plate and the turbulence. Since turbulence can only contribute to a mean velocity in the mean-square or higher correlations, $\bar{\mathbf{u}}'$ is $O(K\epsilon^2\overline{U}_\infty)$. It is convenient to take the free-stream speed $\overline{U}_\infty$ as the unit of velocity, and similarly the density ρ and the plate semi-width b as unity. Therefore, the ith component of the total velocity

$$\mathscr{U}_i = \delta_{1i} + \overline{u}_i + u_{i\infty} + u_i + O(K\epsilon^2)$$

with a corresponding expression for the vorticity.

Assuming that the streamwise integral length scale L_1 of the turbulence is of the same order as the width of the plate, all spatial derivatives, whether of the mean flow or of the turbulence, will be $O(X)$, where X is the quantity differentiated. This assumption excludes the interesting case $L_1 \ll 1$, but rapid-distortion theory cannot be applied to this case with certainty, unless the turbulence is very weak ($\epsilon^{\frac{1}{2}} \ll 1$).

Substituting the expressions for velocity and vorticity into the full vorticity transport equation (the curl of the Navier–Stokes equations), and subtracting those parts satisfied by the mean flow in the absence of turbulence and by the turbulence in the absence of the plate, leaves

$$\left\{\frac{\partial}{\partial t} + \frac{\partial}{\partial x_1}\right\}\boldsymbol{\zeta} + \bar{\mathbf{u}}.\nabla\boldsymbol{\zeta}_\infty + \mathbf{u}_\infty.\nabla\bar{\boldsymbol{\zeta}} = \boldsymbol{\zeta}_\infty.\nabla\bar{\mathbf{u}} + \bar{\boldsymbol{\zeta}}.\nabla\mathbf{u}_\infty + O(K\epsilon^2, K^2\epsilon, K\epsilon R^{-1}). \quad (1)$$

Here $\boldsymbol{\zeta} = \nabla\times\mathbf{u}$, $\boldsymbol{\zeta}_\infty = \nabla\times\mathbf{u}_\infty$ and $\bar{\boldsymbol{\zeta}} = \nabla\times\bar{\mathbf{u}} = (0, 0, \bar{\zeta})$

with $\bar{\zeta} = 0$ outside the wake of the plate. R is the Reynolds number $\overline{U}_\infty b/\nu$, assumed to be large; ν is the kinematic viscosity.

Terms $O(K)$ are small for a sufficiently porous plate, and $\boldsymbol{\zeta}$ and $\mathbf{u}$ are $O(K\epsilon)$, since the largest terms in (1) are of that order. The cross-coupling and inertial transfer terms lumped in the $O(K\epsilon^2, K^2\epsilon)$ bracket are smaller, and may be neglected, as may the viscous terms $O(K\epsilon R^{-1})$, for large Reynolds numbers.

The equation for the undisturbed turbulence is

$$\frac{\partial \boldsymbol{\zeta}_\infty}{\partial t} + \frac{\partial \boldsymbol{\zeta}_\infty}{\partial x_1} = O(\epsilon^2).$$

Neglect of the $O(\epsilon^2)$ inertial transfer terms leaves the 'frozen' turbulence convection equation.

2.2. *The distorted turbulent velocity field*

Expressing the turbulence as a sum of random Fourier components of form $\exp\{i(\omega t - \mathbf{k}.\mathbf{x})\}$, where ω is the frequency and $\mathbf{k}$ the wavenumber of the particular component, and substituting in the above equation for the undisturbed turbulence gives

$$\boldsymbol{\zeta}_\infty = \mathbf{Z}_\infty \exp\{i(\omega t - \mathbf{k}.\mathbf{x})\} + O(\epsilon^2) \quad \text{with} \quad \omega = k_1.$$

$\mathbf{Z}_\infty$ is independent of $\mathbf{x}$ and t, and Fourier transforms are denoted by capital letters.

For the disturbed turbulence,

$$\boldsymbol{\zeta} = \mathbf{Z}(\mathbf{x}) \exp\{i(\omega t - \mathbf{k}.\mathbf{x})\}.$$

This gives, on substitution into (1),

$$\partial \mathbf{Z}/\partial x_1 = i\mathbf{k}.\bar{\mathbf{u}}\mathbf{Z}_\infty - \mathbf{U}_\infty.\nabla\bar{\boldsymbol{\zeta}} + \mathbf{Z}_\infty.\nabla\bar{\mathbf{u}} + \bar{\boldsymbol{\zeta}}.\nabla\mathbf{U}_\infty = ik_1\bar{u}_1\mathbf{Z}_\infty + \boldsymbol{\eta},$$

say. Therefore,

$$\mathbf{Z} = ik_1\left\{\int^{x_1} u_1 dx_1\right\}\mathbf{Z}_\infty + \int^{x_1} \boldsymbol{\eta}\, dx_1.$$

The obvious lower limit for the integrals is $-\infty$, so that $\mathbf{Z} \to 0$ as $x_1 \to -\infty$. But the first integral is divergent in this case for all two-dimensional bodies with significant drag, including porous plates. This is because the perturbation velocity $\bar{u}_1$ decays only like r^{-1} in the far field of a two-dimensional source-like body; hence, anything convected by the perturbed stream from infinitely far upstream suffers a logarithmically infinite delay compared with its time of arrival in the absence of the body.

Darwin (1953) showed that a logarithmic singularity occurred in the drift (the distance travelled with respect to axes fixed in the undisturbed fluid) of material elements along a stagnation streamline. This leads to problems associated with a singularity in the vorticity distibution at a stagnation point, and is discussed by Hunt. But in the present case the drift function is logarithmically singular on all streamlines, owing to the far-field source-like behaviour of the plate. This is associated with the drag of the plate, and occurs for all two-dimensional bodies with significant drag. It is quite distinct from the former effect. The singularity is the same for all streamlines, and induces the same singular phase change in all components of the vorticity; but it does not induce any

amplitude change, nor does it lead to an infinite hydrodynamic mass for such bodies. In reality the phase change is not singular, since the turbulence does not have its origin infinitely far upstream, nor does it perfectly obey Taylor's hypothesis, and the body causing the disturbance cannot be truly two-dimensional.

The significance of the singularity can be seen by considering the equation for the convection of a material quantity χ in a hypothetical flow

$$\bar{\mathbf{q}} = (1+\bar{u}_1, 0, 0).$$

The equation for χ,

$$\frac{\partial \chi}{\partial t} + (1+\bar{u}_1)\frac{\partial \chi}{\partial x_1} = 0,$$

contains the first terms of the vorticity transport equation (1). If, as with the turbulence, χ is considered as a sum of Fourier components so that far upstream where $\bar{u}_1 = 0$,

$$\chi = \mathrm{X}\exp\{i(\omega t - k_1 x_1)\},$$

say, then generally

$$\chi = \mathrm{X}\exp\left\{i\left(\omega t - k_1 x_1 + k_1 \int_{-\infty}^{x_1} \frac{\bar{u}_1 dx_1}{1+\bar{u}_1}\right)\right\}.$$

On expanding the integrand for small $\bar{u}_1$, a term similar to the divergent integral in the expression for $\mathbf{Z}$ is obtained.

So it is apparent that, for $\boldsymbol{\zeta}$ to be small in the region of the plate, it must be defined, not as a perturbation of $\boldsymbol{\zeta}_\infty$ related to an upstream time origin, but as a perturbation of an appropriately delayed $\boldsymbol{\zeta}_\infty(t-\Delta t_\infty)$. Therefore, for a component of frequency ω,

$$\boldsymbol{\zeta} + \boldsymbol{\zeta}_\infty \to \exp\{-i\omega\Delta t_\infty\}\boldsymbol{\zeta}_\infty \quad \text{as} \quad x_1 \to -\infty,$$

far upstream.

Δt_∞ is arbitrary, provided it includes the singular part of the time delay, according to where in the neighbourhood of the plate it is evaluated. It is convenient to calculate Δt_∞ at the point x' at which the velocity $\mathbf{u}$ is required, and at the origin for the drag calculations:

$$\Delta t_\infty = \int_{-\infty}^{x_1'} \bar{u}_1|_{x_2'} dx_1.$$

Since $\boldsymbol{\zeta}$ is now of the same order as $\boldsymbol{\zeta}_\infty$ at $x_1 = -\infty$, the small-perturbation equation (1) is not valid up to this limit, and the upstream boundary condition must be applied at an intermediate limit. We choose this as $\bar{x}_1 = -\mathrm{X}_1/K$, with X_1 fixed and positive so that $\bar{x}_1 \to -\infty$ as $K \to 0$.

The solution of (1) for $\mathbf{Z}$, satisfying the boundary condition at this limit, omitting terms of order $(K^2\epsilon)$ is

$$\mathbf{Z} = ik_1\left\{\int_{-\infty}^{x_1} \bar{u}_1 dx_1 - \Delta t_\infty\right\}\mathbf{Z}_\infty + \int_{-\infty}^{x_1} \boldsymbol{\eta}\, dx_1.$$

As $x_1 \to -\mathrm{X}_1/K$,

$$\begin{aligned}\boldsymbol{\zeta} + \boldsymbol{\zeta}_\infty - \exp\{-i\omega\Delta t_\infty\}\boldsymbol{\zeta}_\infty \to{}& [1 - i\omega\Delta t_\infty - \exp\{-i\omega\Delta t_\infty\}]\boldsymbol{\zeta}_\infty \\ &+ ik\int_{-\infty}^{-\mathrm{X}_1/K} \bar{u}_1 dx_1 \boldsymbol{\zeta}_\infty + \int_{-\infty}^{-\mathrm{X}_1/K} \boldsymbol{\eta}\, dx_1 \\ &\to 0 \quad \text{as} \quad K \to 0.\end{aligned}$$

So this also satisfies the upstream boundary condition. But the vorticity equation does not hold across the plate, so that the solution for $\mathbf{Z}$ downstream in the wake of the plate may contain an additional constant of integration $\mathbf{Z}_w(x_2)$, say.

Therefore, since $\bar{\mathbf{u}} = (\bar{u}_1, \bar{u}_2, 0)$ and $\bar{\boldsymbol{\zeta}} = (0, 0, \bar{\zeta})$,

where $\bar{\zeta}$ is a function of x_2 only to order (K) for $x_1 > 0$ and is zero for $x_1 < 0$, the components of the vorticity perturbation $\mathbf{Z}$ can be written as

$$\left.\begin{aligned}
\mathrm{Z}_1 &= \{I(\bar{\mathbf{u}}) + \bar{u}_1\}\mathrm{Z}_{1\infty} + \bar{u}_2\mathrm{Z}_{2\infty} - \bar{\zeta}x_1 H(x_1)\{\mathrm{Z}_{2\infty} + ik_3 U_{1\infty}\} + \mathrm{Z}_{1w}(x_2)H(x_1),\\
\mathrm{Z}_2 &= \{I(\bar{\mathbf{u}}) - \bar{u}_1\}\mathrm{Z}_{2\infty} + \bar{u}_2\mathrm{Z}_{1\infty} - \bar{\zeta}x_1 H(x_1)\{ik_3 U_{2\infty}\} + \mathrm{Z}_{2w}(x_2)H(x_1),\\
\mathrm{Z}_3 &= I(\bar{\mathbf{u}})\mathrm{Z}_{3\infty} - \frac{\partial\bar{\zeta}}{\partial x_2}x_1 H(x_1)U_{2\infty} - \bar{\zeta}H(x_1)U_{1\infty} - \bar{\zeta}x_1 H(x_1)\{ik_3 U_{3\infty}\} + \mathrm{Z}_{3w}(x_2)H(x_1).
\end{aligned}\right\} \tag{2}$$

Here, $$I(\bar{\mathbf{u}}) = ik_1\left\{\int_{x_1'}^{x_1}\bar{u}_1\,dx_1 + \int_{-\infty}^{x_1'}(\bar{u}_1 - \bar{u}_1|_{x_2'})\,dx_1\right\} + ik_2\int_{-\infty}^{x_1}\bar{u}_2\,dx_1,$$

and $H(x_1) = 0$ outside and 1 inside the wake of the plate.

Because (1) does not hold through the plate, where a jump in the value of the vorticity occurs, the vorticity in the wake is as yet only specified to within the arbitrary constant of integration $\mathbf{Z}_w(x_2)H(x_1)$. This term represents the additional vorticity generated by the fluctuating pressure drop across the plate, as a result of which the turbulence far downstream even in the idealized wake of the plate does not return to its undisturbed state. Boundary conditions at the plate are required to specify $\mathbf{Z}_w$.

Viewed on the scale of the lattice or hole structure of the plate, Z_w is the change in vorticity that occurs when the structure of the plate interrupts incident vortex lines by stretching and dissipation near the surface, and adds to the vorticity by shedding from the edges. Viewed on the scale of the plate, the change in vorticity is associated with the blocking action of the plate and its resistance to the flow through it. The other discontinuous terms in the expression for $\mathbf{Z}$ result from interactions between the fluctuating flow and the mean wake vorticity. Therefore, the total unsteady vorticity field can be divided into three parts: (i) $\boldsymbol{\zeta}_\infty$, the undisturbed incident vorticity; (ii) $\boldsymbol{\zeta}_w$, consisting of the discontinuous terms in (2) which contain the factor $H(x_1)$ and are zero outside the wake; (iii) $\boldsymbol{\zeta}' = \boldsymbol{\zeta} - \boldsymbol{\zeta}_w$, the remainder, continuous across the plane of the plate.

It is the fluctuating velocity, rather than the vorticity near the plate, that is of interest. The velocity field, expressed in terms of components corresponding to (i)–(iii), is

$$\mathbf{u}_\infty + \mathbf{u}' + \mathbf{w} + \nabla\phi \quad \text{where} \quad \nabla\times\mathbf{u}_\infty = \boldsymbol{\zeta}_\infty, \quad \nabla\times\mathbf{u}' = \boldsymbol{\zeta}' \quad \text{and} \quad \nabla\times\mathbf{w} = \boldsymbol{\zeta}_w.$$

ϕ is an arbitrary potential, determined by boundary conditions and satisfying $\nabla^2\phi = 0$. The rotational wake velocity $\mathbf{w}$ can be defined to be zero outside the wake without loss of generality, by including any irrotational velocity field associated with $\boldsymbol{\zeta}_w$ in $\nabla\phi$. The vortex lines of $\boldsymbol{\zeta}'$ are continuous everywhere; therefore, since $\nabla.\mathbf{u}' = 0$, $\mathbf{u}'$ can be calculated from the Biot–Savart integral

$$\mathbf{u}'(\mathbf{x}') = -\iiint_{-\infty}^{\infty}\frac{\boldsymbol{\zeta}'\times(\mathbf{x}-\mathbf{x}')}{4\pi|\mathbf{x}-\mathbf{x}'|^3}\,dx_1\,dx_2\,dx_3. \tag{3}$$

2.3. *The boundary conditions at the plate*

Application of the momentum equation to both sides of the plate gives the equation for the pressure difference Δp across the plate

$$\nabla(\Delta p) = \mathscr{U} \times (\bar{\boldsymbol{\zeta}} + \boldsymbol{\zeta}_w) - \Delta\{\partial \mathscr{U}/\partial t + \tfrac{1}{2}\nabla \mathscr{U}^2\} + O(R^{-1}), \tag{4}$$

in which $\mathscr{U}$, the total instantaneous velocity, is continuous across the plate in order to satisfy continuity of flow and the assumption of no refraction. Δ is the normal jump across $x_1 = 0$: {side (2) > 0 − side (1) < 0}. The pressure jump is also related to the velocity at the plate by the resistance equation

$$\Delta p = \tfrac{1}{2} K \mathscr{U}^2. \tag{5}$$

Eliminating Δp between (4) and (5) gives an equation which specifies the jump in $\boldsymbol{\zeta}_w$ at the plate, and hence $\mathbf{Z}_w$ in (2). Integrating this in the x_2 direction from $-\infty$, with $\boldsymbol{\zeta}_w$ expressed as $\nabla \times \mathbf{w}$, gives to $O(K\epsilon)$, for the fluctuating part,

$$\frac{D}{Dt}\{\phi_1 - \phi_2\} = \frac{-2K}{4+K}(u_1' + u_{1\infty}) + \int_{-1}^{x_2} \frac{Dw_2}{Dt}\, dx_2|_{x_1=0}. \tag{6}$$

In (6) values for $\bar{u}_1$ are substituted from Taylor's solution for the mean flow, and

$$\frac{D}{Dt} \equiv \frac{\partial}{\partial t} + \frac{4}{4+K}\frac{\partial}{\partial x_1}.$$

The latter is the convective derivative corresponding to the mean velocity through the plate. ϕ_i is the fluctuating part of the potential on side i of the plate. From above,

$u_1 = \partial\phi_i/\partial x_1 +$ the Biot–Savart perturbation component $+ w_1$ (in the wake).

On the upstream side,

$$u_1 = u_1'' + \partial\phi_1/\partial x_1 - u_{1\infty}$$

say, where u_1'' is the total fluctuating normal velocity component 'felt' by the plate. A second boundary-value equation is required to fix ϕ_1 and ϕ_2. Continuity of the fluctuating part of $\mathscr{U}$ at the plate gives

$$\nabla\phi_1 = \nabla\phi_2 + \mathbf{w}|_{x_1=0,\,|x_2|\leqslant 1}.$$

But $\nabla w = 0$ and $\nabla^2\phi_i = 0$ by continuity; therefore,

$$\frac{D}{Dt}\left(\frac{\partial\phi_1}{\partial x_1} - \frac{\partial\phi_2}{\partial x_1}\right) = \frac{Dw_1}{Dt}\,|_{x_1=0,\,|x_2|\leqslant 1}. \tag{7}$$

The potential ϕ is $O(K\epsilon)$. Since $\boldsymbol{\zeta}_w$ satisfies $D\boldsymbol{\zeta}_w/Dt = 0$ to $O(K\epsilon)$, Dw/Dt on the right-hand sides of (6) and (7) is $O(K^2\epsilon)$ at most, and may be neglected in calculating ϕ to $O(K\epsilon)$. However, the resulting equations still contain some higher-order ($K^2\epsilon$) terms, which have been retained, to preserve compatibility with similar higher-order terms in Taylor's theory. It is these terms that enable the theory to give reasonable predictions of the mean drag coefficient up to $K = 4$, and of the mean velocity field for all K. Without them the theory is only applicable for $K \ll 4$. But the Dw/Dt terms on the right-hand sides of (6) and (7)

greatly increase the difficulty of obtaining a solution, and do not relate to Taylor's mean flow theory. In Graham (1972, appendix B) they were shown to be of order $(kK\epsilon\overline{u}_2)$. They are e.g. very small in both the cases of very large scale and very small scale turbulence. $\overline{u}_2$ is much less than $\overline{u}_1$ over most of the plate, and terms of this order $(\overline{u}_2)$ are neglected in Taylor's theory, being also of the order of the difference between the various different formulae proposed for pressure drop and refraction equations across gauzes and porous plates. They will therefore be assumed to be small enough to be neglected in the present analysis.

The two equations (6) and (7) for ϕ_i only apply within the area of the plate $|x_2| \leqslant 1$. Outside the plate, $(\phi_1 - \phi_2)$ and all its higher derivatives with respect to x_1 are zero on $x_1 = 0$, in order to satisfy continuity of velocity and pressure.

Combining these with (6) and (7), and writing $\beta = 4/(4+K)$, the potential flow problem for ϕ_1 and ϕ_2 becomes

$$\nabla^2\phi_1 = \nabla^2\phi_2 = 0, \tag{8}$$

$$\left\{\frac{\partial}{\partial t} + \beta\frac{\partial}{\partial x_1}\right\}\{\phi_1 - \phi_2\} = -\tfrac{1}{2}K\beta\left(u_1'' + \frac{\partial\phi_1}{\partial x_1}\right)\Big|_{x_1=0,|x_2|\leqslant 1} = 0\,\Big|_{x_1=0,|x_2|>1}, \tag{9}$$

$$\left\{\frac{\partial}{\partial t} + \beta\frac{\partial}{\partial x_1}\right\}\frac{\partial}{\partial x_1}\{\phi_1 - \phi_2\} = 0\Big|_{x_1=0,\,\text{all } x_2}. \tag{10}$$

If the flow is steady ($k_1 = 0$), these equations reduce to

$$\frac{\partial\phi_1}{\partial x_1} = -\frac{\partial\phi_2}{\partial x_1} = -\frac{K}{4+K}u_1'' \quad \text{on} \quad x_1 = 0, \quad |x_2| \leqslant 1,$$

which is identical with Taylor's steady flow equation. In this case, Vickery's quasi-steady formula applies for the drag, provided the calculation is based on the incident velocity u_1'', which includes the effect of distortion by the mean flow. Also, for every small K, the loading on the plate at all frequencies is $\Delta p = Ku_\infty + O(K^2)$, which, neglecting the $O(K^2)$ terms, is the relationship assumed by Vickery.

2.4. *Calculation of unsteady drag and velocity spectra*

Equations (8)–(10) were solved by a Fourier transform method described in appendix A. The drag was obtained in the form

$$D = U_1'' P_0(\mathbf{k}) \exp[i(\omega t - k_3 x_3)]$$

with a similar solution for the upstream velocity component $\partial\phi_1/\partial x_1$. In appendix B, the distorted turbulent velocity field u_1' is expressed in the form

$$u_1' = U_{j\infty}\left\{\exp[-i(k_1x_1 + k_2x_2)]\,\delta_{ij} + \frac{4K}{4+K}\int_0^\infty \frac{\sin\lambda}{\pi\lambda}F_j(\lambda, \mathbf{x})\,d\lambda\right\}\exp[i(\omega t - k_3x_3)]. \tag{11}$$

We are therefore in a position to calculate details of the velocity and pressure field in the vicinity of the plate, provided an adequate description of the upstream turbulence can be obtained. The simplest and perhaps the most important quantity both to measure and calculate is the overall unsteady drag of the plate.

The expression $F(\lambda)$ contains terms in $\exp(-ik_2x_2)$ and $\exp[-i(k_2\pm\lambda)x_2]$; therefore (11) has the form of a scattering relation for 'breadth-wise', (2-) wavenumber, components. That is, when a component of wavenumber k_2 is incident on the plate, the effect of the plate's mean velocity field is to scatter this into a continuous spectrum of (2-) wavenumbers which constitute the Biot–Savart distortion field. The potential flow solution for the unsteady drag is of the form

$$D = U_1''|_{x_1=0} P_0(\mathbf{k}) \exp[i(\omega t - k_3 x_3)] \tag{12}$$

for each incident streamwise velocity component $U_1'' \exp[i(\omega t - \mathbf{k}.\mathbf{x})]$ 'felt' by the plate. There is no dependence on transverse components. The general form of $\mathbf{F}(\lambda)$ on $x_1 = 0$ is

$$\mathbf{f}_1(\lambda)\exp(-ik_2x_2) + \mathbf{f}_2(\lambda)\exp[i(k_2-\lambda)x_2] + \mathbf{f}_3(\lambda)\exp[-i(k_2+\lambda)x_2].$$

The drag response to each (2-) wavenumber component can be evaluated separately and the result integrated over λ. Therefore, the fluctuating drag induced on the plate by a *free-stream* component of turbulence

$$\mathbf{U}_\infty \exp[i(\omega t - \mathbf{k}\cdot\mathbf{x})],$$

including the effects of distortion, is

$$\begin{aligned} D = \exp[i(\omega t - k_3x_3)]\Bigg\{U_{1\infty}\Bigg[P_0(\mathbf{k}) + \frac{4K}{4+K}\int_0^\infty \frac{\sin\lambda}{\pi\lambda}\Big\{f_{11}(\lambda)\,P_0(\mathbf{k}) \\ + f_{21}(\lambda)\,P_0(k_1, k_2-\lambda, k_3) + f_{31}(\lambda)\,P_0(k_1, k_2+\lambda, k_3)\Big\}\,d\lambda\Bigg]\Bigg\} \\ + \text{similar terms involving } U_{2\infty} \text{ and } U_{3\infty}. \end{aligned} \tag{13}$$

For simplicity, let

$$D = \mathrm{X}_j U_{j\infty} \exp[i(\omega t - k_3 x_3)]. \tag{14}$$

Equation (14) is an expression relating the random variables D, the sectional drag, and $U_{j\infty}$, the velocity wavenumber components. This relationship can be used, e.g., to express the measurable quantity $S_{DD}(\omega, s)$, the frequency spectrum of drag on a rectangular element of the plate of spanwise length $2s$, in terms of the triple wavenumber spectrum tensor $\mathbf{S}_{ij}(\mathbf{k})$ of the turbulence.

Following the analysis of Roberts (1971) and others,

$$S_{DD}(\omega) = 16s^2 \iint_{-\infty}^{\infty} \mathbf{S}_{ij}(\mathbf{k}) \langle \mathrm{X}_i \mathrm{X}_j^*(\mathbf{k}) \rangle \frac{\sin^2 k_3 s}{(k_3 s)^2}\, dk_2 dk_3. \tag{15}$$

$*$ denotes the complex conjugate. If further we assume that the undistorted turbulence is isotropic,

$$\mathbf{S}_{ij}(\mathbf{k}) = \left(\frac{\delta_{ij}k^2 - k_i k_j}{k_2^2 + k_3^2}\right)\mathbf{S}_{11}(\mathbf{k}) = p_{ij}\,\mathbf{S}_{11},$$

say. Therefore,

$$S_{DD}(\omega) = 64s^2 \int_0^\infty \int_0^\infty \mathbf{S}_{11}(\mathbf{k})\, p_{ij} \langle \mathrm{X}_i \mathrm{X}_j^* \rangle \sin^2 k_3 s/(k_3 s)^2\, dk_2 dk_3. \tag{16}$$

A convenient way of describing the overall unsteady forces induced on a body in a particular turbulent flow is by making use of the concept of an aerodynamic admittance function for that force. Using Davenport's (1961) definition,

$$A(\omega) = S_{DD}(\omega)/\{16s^2C_D^2 S_{11}(\omega)\}. \tag{17}$$

The mean drag coefficient $C_D = K/(1+\frac{1}{4}K)^2$ in this case. Therefore, substituting from (16) with isotropic turbulence,

$$A(\omega) = \frac{4(1+\frac{1}{4}K)^2}{K^2}\int_0^\infty\int_0^\infty \frac{\mathbf{S}_{11}(\mathbf{k})}{S_{11}(\omega)} P_{ij}\langle \mathrm{X}_i \mathrm{X}_j^*\rangle \frac{\sin^2 k_3 s}{(k_3 s)^2}\, dk_2 dk_3. \tag{18}$$

Similarly, it is possible to calculate the spectrum of the distorted turbulence field in the neighbourhood of the plate. For example, along the upstream centreline, the distorted streamwise velocity spectrum, including the potential or blockage part of the velocity field, is

$$S'_{11}(\omega)|_{x_2=0} = 4\int_0^\infty\int_0^\infty \mathbf{S}_{11}(\mathbf{k})\, p_{ij}\langle Y_i Y_j^*\rangle\, dk_2 dk_3, \tag{19}$$

where $$Y_j = \delta_{1j}\exp(-ik_1x_1) + \frac{4K}{4+K}\int_0^\infty \frac{\sin\lambda}{\pi\lambda} F_j(\lambda, x_1)\, d\lambda + \partial\phi_1/\partial x_1|_{x_2=0}.$$

Three-dimensional plates can be analysed by an extension of the above analysis.

3. Experimental measurements

3.1. *Description of the turbulence*

It is generally assumed, with some experimental justification (e.g. Roberts 1971), that grid turbulence at order ten mesh lengths downstream of the grid is both reasonably isotropic in its length scales, and quite well described by the von Kármán spectrum at all but the very highest and perhaps lowest frequencies. This spectrum, or part of it, is also found to describe certain atmospheric conditions adequately. However, it must be emphasized that in none of the theories for turbulent loading is it necessary to assume the von Kármán spectrum. All that is required is an adequate description of the undisturbed turbulence in the particular situation being modelled. The longitudinal von Kármán spectrum at frequency n (Hz) is

$$S_{11}(n) = \frac{4\overline{u}_{1\infty}^2 L_1}{\overline{U}_\infty}\left\{1 + 4\pi\frac{\Gamma^2(\frac{1}{3})\, L_1^2 n^2}{\Gamma^2(\frac{5}{6})\overline{U}_\infty^2}\right\}^{-\frac{5}{6}}.$$

Harris (1970) deduced from this an expression for the triple wavenumber spectrum for an isotropic turbulence, which can be expressed as

$$\mathbf{S}_{11}(\mathbf{k}) = \frac{55\sigma^5(k_2^2+k_3^2)}{9\pi(\sigma^2+|\mathbf{k}|^2)^{\frac{17}{6}}} L_1 \overline{u}_{1\infty}^2,$$

where $$\sigma = \pi^{\frac{1}{2}}\Gamma(\tfrac{5}{6})/[\Gamma(\tfrac{1}{3})L_1].$$

This spectrum is not in itself a measurable quantity, but an integrated Fourier transform of it, the coherence function

$$\mathbf{R}_{11}(k_1, y) = \frac{1}{(2\pi)^{\frac{1}{2}}} \iint_{-\infty}^{\infty} \mathbf{S}_{11}(\mathbf{k}) \exp(-ik_2 y)/S_{11}(\omega)\, dk_2 dk_3$$
$$= \frac{2}{\Gamma(\frac{5}{6})} \left\{ \left(\frac{y'}{2}\right)^{\frac{5}{6}} K_{\frac{5}{6}}(y') - \left(\frac{y'}{2}\right)^{\frac{1}{6}} K_{\frac{1}{6}}(y') \right\},$$

where $y' = y(\sigma^2 + k_1^2)^{\frac{1}{2}}$ is measurable.

Bearman (1969) showed how Vickery's admittance formula can be expressed as a double integral involving this coherence function. Therefore, measurements of it are clearly a useful test of the adequacy of the description of the turbulence. Harris (1970) and Roberts (1971) compared the function with grid turbulence data.

The present experiments were carried out using various biplanar grids to generate the turbulence, which was assumed to be well approximated over the energetic regions by the above formulae. Figure 7 compares the empirical with a measured, one-dimensional longitudinal spectrum. The appropriate length scales were calculated from the zero-frequency intercepts of the spectra.

3.2. *Measurements of the drag-admittance of porous plates*

A series of wind-tunnel experiments was conducted, to measure the effect of the resistance K on the admittance of various two-dimensional and square plates downstream of a turbulence grid. The plates were of two types: (i) a wire gauze stretched over a skeleton framework, giving a drag coefficient of 0·62; (ii) various thin plastic plates drilled with a square pattern of round holes, three holes across the width of the plate, giving drag coefficients from 0·54 to 1·20. The plates were mounted on stings connecting them with a piezo-electric drag balance. Figure 4 shows a typical spectrum of drag. The prominent peak is the mechanical resonance of the system. Graham (1972) describes the experimental arrangements more fully.

The plates were positioned ten and fourteen mesh lengths downstream of the grid used. The experimental details are listed in table 1. In the cases of two-dimensional plates, it was necessary to have two small gaps separating the square sensing element from the rest of the plate. This permitted a small extra through-flow, which increased the effective porosity of the plate. An estimated porosity correction was made to take this into account, by adding half the open area of the gaps to the open area of the element. But, for the same reason, no two-dimensional solid plate measurements were made, since it was felt that the gaps would have a considerable effect on the near-wake region.

The blockage-area ratio was less than 4% for all the plates and, since in defining admittance a ratio of fluctuating to mean drag is used, no blockage corrections were applied.

The resistance coefficients of the gauze structure, and the various plate/hole geometries were measured by placing samples completely across a duct. Some underestimate of K is probable, using this method, because of boundary-layer effects.

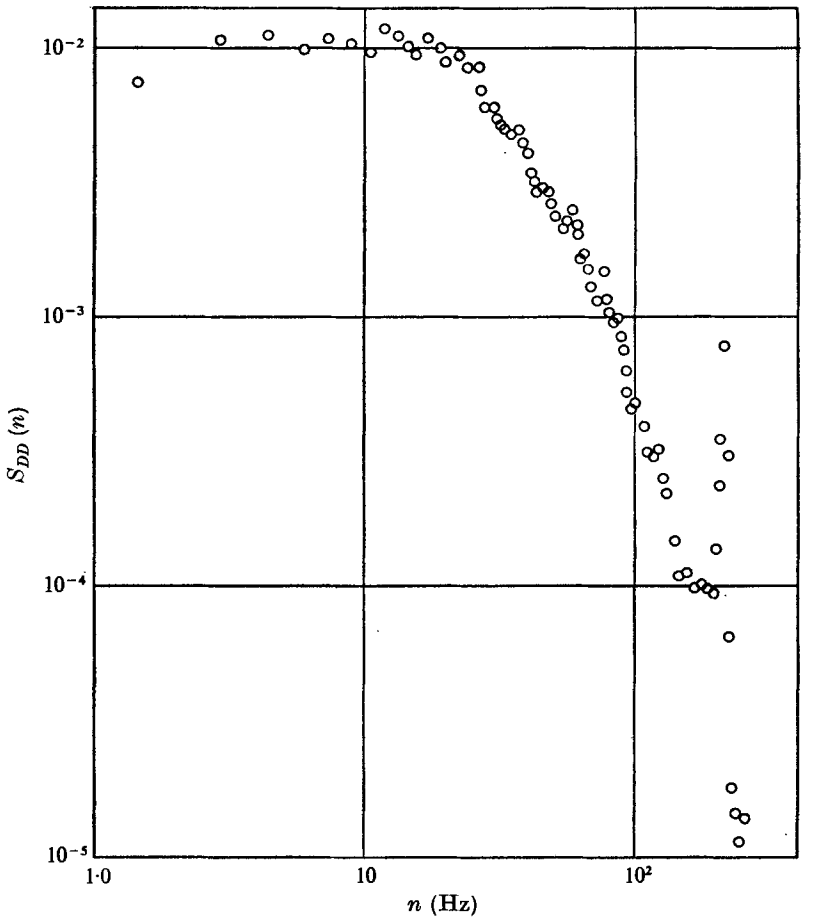

FIGURE 4. Spectrum of drag of a square plate.

	β	K	M	b/M	X/M	$R_b \times 10^{-4}$
Gauze						
1	0·58	1·3	152	0·33	10	5
2	0·58*	1·3	152	0·33	10	5
Round holes						
3	0·62	1·2	32	0·57	14	2
4	0·62*	1·2	32	0·57	14	2
5	0·48	4·5	32	0·57	14	2
6	0·48*	4·5	32	0·57	14	2
7	0·34	11·0	32	0·57	14	2
8	0·34*	11·0	32	0·57	14	2
9	0·23	22·5	32	0·55	14	2
10	0·23*	22·5	32	0·55	14	2
Solid						
11	0	∞	32	0·57	14	2

TABLE 1. Experimental details. Open-area ratio β; resistance coefficient K; β and K uncorrected for gap effect; *, two-dimensional configuration. Mesh size of turbulence grid M (mm); distance of plate downstream of grid X; nominal Reynolds number based on the plate semi-width b.

The mean drag coefficients of the plates were all measured in a turbulent incident flow. They are plotted against open-area ratio β and resistance coefficient K in figure 2. The main conclusion from comparing these results with those of other experiments is that square isolated plates have a consistently lower drag coefficient than two-dimensional plates of the same porosity, although the difference is very small at high porosities. The comparison with Taylor's theory indicates that it gives a reasonable estimate of the drag up to values of K in the region of 4. There is little conclusive evidence of the effect of turbulence on the drag coefficients, except perhaps at zero porosity.

3.3. *Measurement of velocity spectra on the centre-line*

Some measurements of the distorted turbulent velocity field ahead of the plates were also taken. The intensity and spectra of the streamwise component were measured with a hot-wire probe on the centre-line ($x_2 = 0$). The probe was aligned with the flow, and traversed through a hole in the centre of the plate. This hole was made larger than the other holes in the porous plate, to compensate for the blockage of the probe stem.

Measurements were made between 0·125 and 2·5 plate diameters upstream. Those closest to the plate were at a distance from the plate similar to the hole size, and showed some effect of the non-homogeneity of the porosity on the mean velocity (figure 3). Elsewhere there was good agreement with Taylor's theory.

The turbulence was also measured in the absence of the plate (referred to as $K = 0$), and, in the case of the smallest scale, showed an appreciable decay over the streamwise range of the measurements. By measuring the distortion relative to the undistorted turbulence *at the same streamwise station* reasonable agreement was obtained between theory and experiment. This suggests that rapid-distortion theory may be applied to fairly small length scales, provided decay is taken into account in this way, as Tucker & Reynolds (1968) found for homogeneous strain fields.

The theoretical predictions were much less sensitive to the small changes in length scale of the convected turbulence over the measurement range, and all calculations were therefore based on a nominal value of length scale for each grid.

4. Discussion of the numerical results and comparison with experiment

4.1. *Drag spectra (admittance)*

Figure 5 shows the calculated and measured values of admittance for the element of a two-dimensional gauze plate. The corresponding three-dimensional (square plate) case is shown in the same figure. At these low values of K and L_1^{-1}, there is not much difference between the $K = 0$ (Vickery) theory and the results of the present theory for the square porous plate and the square element in a two-dimensional plate.

In order to try to obtain a more decisive measurement of the effect of K on the admittance, the more extensive series of tests using drilled plastic plates was carried out. In this case the grid used was also sufficiently small to give a value of L_1 lower than in the previous experiment. The results are plotted in

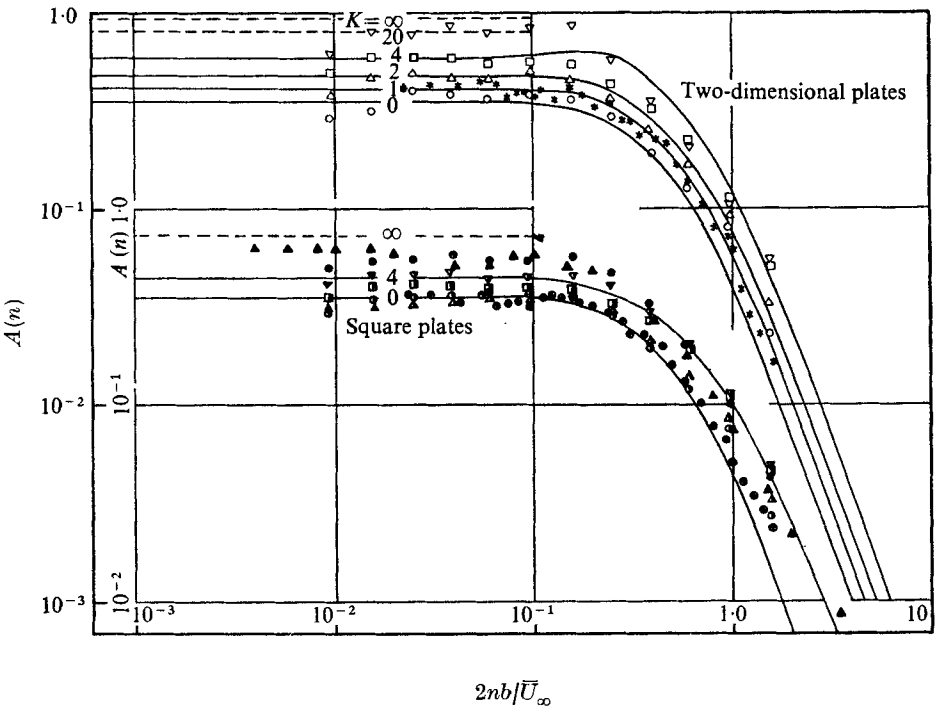

FIGURE 5. Admittances of plates of varying resistance. Theory: ——, $L_1 = 0{\cdot}75$, values of K on the curves; – – –, $K = \infty$ (solid plate) and 20 (near-solid). Experiment as follows. Gauze, $L_1 = 1{\cdot}25$, $K = 1{\cdot}0$: *, two-dimensional; ⊕, square. Solid, $K = \infty$, square: ●, $L_1 = 0{\cdot}816$; ▲, $L_1 = 0{\cdot}75$, Bearman (1969). Otherwise as follows, for $L_1 = 0{\cdot}816$.

	Two-dimensional				Square			
K	1·0	3·3	7·6	16·2	1·4	4·4	10·9	22·4
	○	△	□	▽	◑	◭	◨	▼

figure 5, and the comparison with results computed from the theory shows the same trend of increasing admittance with increasing K and a reasonable measure of agreement in the absolute values of the admittances.

The theory clearly breaks down as $K \to \infty$ (e.g. the mean drag coefficient $\to 0$ and the admittance, for $k_1 \neq 0, \to \infty$), and is probably reasonable only for $K \leqslant 4$. Theoretical admittances are also plotted in figure 6 for two-dimensional plates of fixed $K\,(=4)$, but with varying length scales L_1 of the turbulence. The main effect of the distortion correction at low frequencies is to raise all the admittances differentially, with the biggest effect for the smallest L_1, bringing them closer together.

4.2. *Centre-line velocity spectra and intensities*

Figure 7 shows calculated and measured spectra at one quarter of a plate diameter ahead of the plate, close to the point of maximum streamwise intensity for the smaller length scale. Nearer the plate, the intensity of this component is reduced by the dominant blocking action of the plate. Asymptotic spectra (see §4.3, (iv)), for zero length scale turbulence that undergoes no blocking ahead of the plate, are also plotted in the figure. Comparison of the spectra indicates that blocking is significant only at the low frequency end of the spectrum,

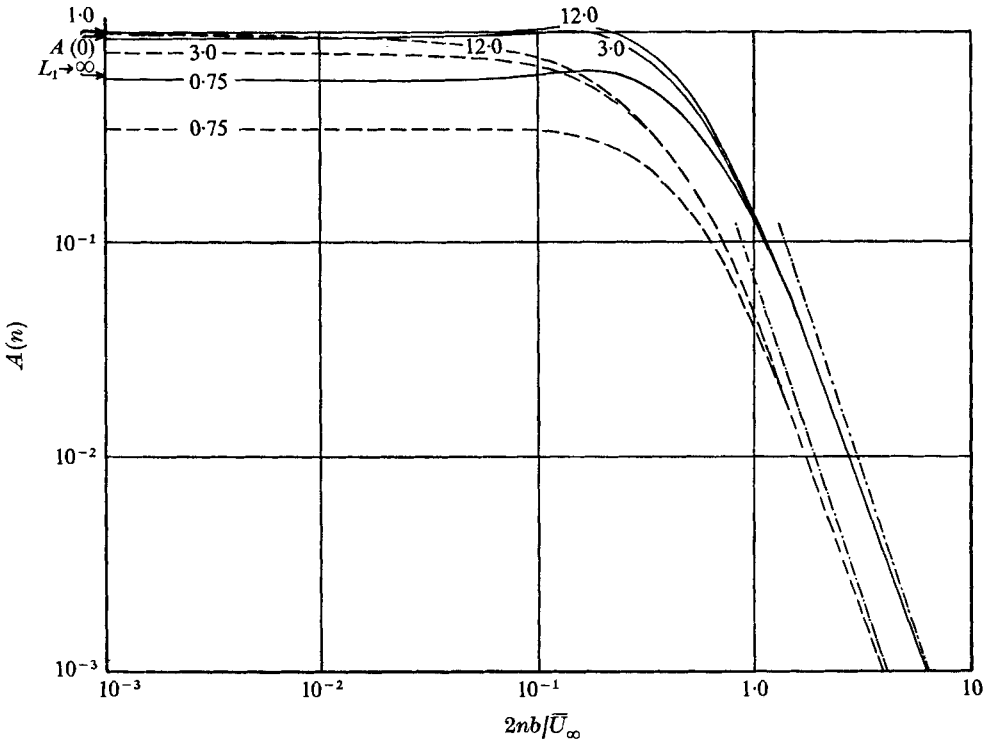

FIGURE 6. Calculated admittances of two-dimensional plates in turbulence of different length scales. Values of L_1 on the curves: ——, $K = 4$; – – –, 0. —·—·—, asymptotes for high frequencies.

$n < n_0$, where n_0 is very approximately independent of the length scale of the turbulence for the cases shown. The reduced effect of blocking at high frequencies has also been demonstrated in other experiments (e.g. Bearman 1971), and is associated with the rapid fall-off in the potential flow field at high frequency.

For sufficiently high frequency, the linearized theory (see §4.3) predicts that the effects of distortion become independent of the length scale of the turbulence, and the distorted spectrum tends to a constant multiple of the undistorted spectrum:

$$S'_{11}(n) \to \{1 + \tfrac{4}{17}(1 - \overline{\mathscr{U}}_1)\} S_{11}(n).$$

$\overline{\mathscr{U}}_1 = 1 + \overline{u}_1$ is the total mean streamwise velocity. However, although both the linearized theory and Hunt's full theory predict an increase in the spectrum at high frequencies, the measurements show an appreciable decrease. (See also Bearman 1971.) It is probable that this is associated with increased dissipation in the intensified turbulence ahead of the plate, since, the greater the intensification at low frequencies, the greater the fall in the spectrum at high frequencies.

Figure 8 shows predicted and measured intensities of the streamwise velocity on the centre-line. Measurements and some calculated results have also been included for the solid plate ($K = \infty$). It is clear from these results that the linearized theory *underestimates* the degree of distortion occurring ahead of the plate, particularly in regions where $|\overline{\mathscr{U}}|$ is $O(1)$. For this reason, the theoretical curve for $K = \infty$ has not been calculated closer to the plate than half a diameter.

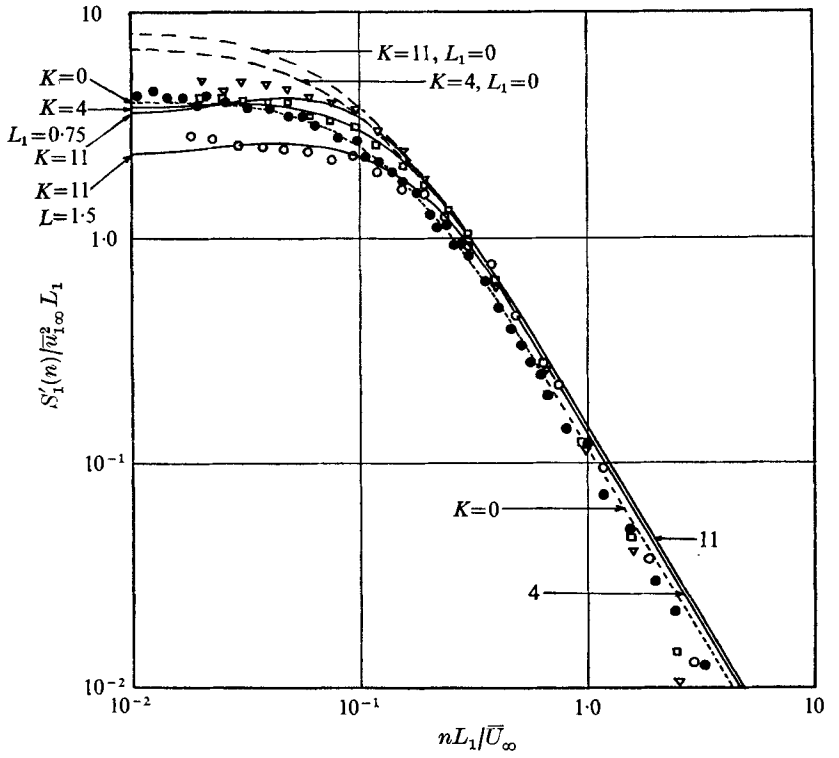

FIGURE 7. Velocity spectra on upstream centre-line of two-dimensional plates, $K_1 = -0{\cdot}5$. - - -, von Kármán spectrum (undistorted). ——, spectrum given by linearized distortion theory, values of K and L_1 on the curves. – – –, asymptotic spectra for $L_1 \to 0$. Experiment: ●, no plate, $L_1 = 0{\cdot}816$; otherwise as follows:

K	4·5	11·0	11·0
L_1	0·816	0·816	1·67
	□	▽	○

4.3. *Asymptotic behaviour (two-dimensional plates)*

(i) *Low frequency.* As $k_1 \to 0$ with all other parameters fixed, the $\partial/\partial t$ terms in (8) and (9) associated with acceleration become negligible. The resulting equations lead to Vickery's formula for the drag, D_v say. In this case, the calculated increase in the admittance comes entirely from distortion of the turbulent velocity field.

(ii) *High frequency.* When k_1 is very large the main contribution to the integrals in (18) and (19) occurs when k_2 and k_3 are correspondingly large. The distortion function $F_j(\lambda)$ has the asymptotic form on $x_2 = 0$, for large k/λ,

$$F_j(\lambda/k \to 0) = \left\{\left(\tfrac{1}{2} + \frac{k_2^2 - k_1^2}{k^2}\right)\left(\delta_{ij} - \frac{k_1 k_j}{k^2}\right) - e_{3jq}\frac{k_2 k_q}{k^2}\right\} \exp\left[(\lambda - ik_1)x_1\right].$$

This is independent of λ/k and hence of L_1. Integrating (19) gives the velocity spectrum

$$S'_{11}(n) = \{1 + \tfrac{4}{17}(1 - \overline{\mathscr{U}}_1)\} S_{11}(n).$$

In the potential equation for the drag, the $\partial/\partial t$ terms dominate, leading to

$$D = (1 + \tfrac{1}{4}K) D_v.$$

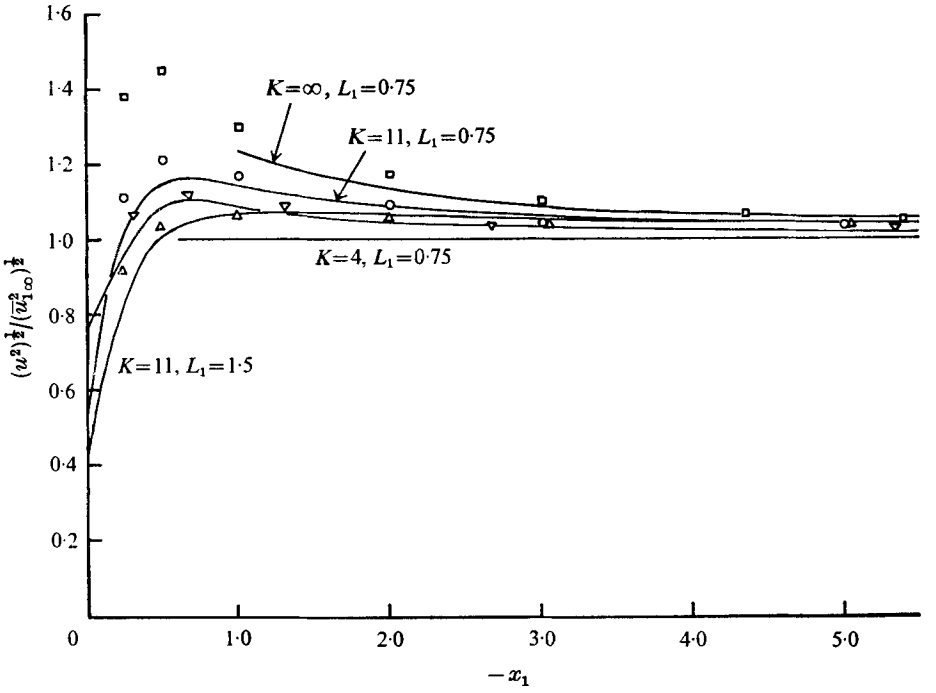

FIGURE 8. Turbulence intensity on the centre-line. ——, theory, values of K and L_1 on the curves. Experiment as follows:

K	4·5	11·0	11·0	∞
L_1	0·816	0·816	1·67	0·816
	∇	$\bigcirc$	$\triangle$	$\square$

D_v is Vickery's formula for the drag. Combining this with the velocity distortion formula above, and using Roberts' (1971) high frequency asymptote for D_v with a von Kármán turbulence spectrum, gives

$$A(n) \to 1{\cdot}86\{1+0{\cdot}559K+0{\cdot}077K^2\}\{\sigma^2+4\pi^2n^2\}^{-\frac{5}{6}}, \quad \text{where} \quad \sigma = \pi^{\frac{1}{2}}\Gamma(\tfrac{5}{6})/(\Gamma(\tfrac{1}{3})\,L_1).$$

This asymptote is shown in figure 6.

(iii) *Large length scale turbulence* ($L_1 \to \infty$). Equation (16) for the spectrum of unsteady drag can be rewritten as

$$S_{DD}(\omega) = \frac{880 L_1 \overline{u}_{1\infty}^2 s^2 \sigma^{\frac{5}{3}}}{9\pi\gamma^{\frac{5}{3}}} \int\int_{-\infty}^{\infty} \frac{(\delta_{ij}\hat{k}^2 - \hat{k}_i\hat{k}_j)}{(1+\hat{k}_2^2+\hat{k}_3^2)^{\frac{17}{6}}} \langle \mathrm{X}_i \mathrm{X}_j^*(\gamma\hat{k})\rangle \frac{\sin^2\gamma\hat{k}_3 s}{(\gamma\hat{k}_3 s)^2} d\hat{k}_2 d\hat{k}_3,$$

where $$\hat{k}_i = k_i/\gamma \quad \text{and} \quad \gamma = (\sigma^2+k_1^2)^{\frac{1}{2}}.$$

If we now let $L_1 \to \infty, \sigma \to 0$, and if k_1 is held fixed $\neq 0$ (i.e. ω is fixed), $S_{DD} \to 0$, because the frequency parameter $k_1 L_1$ is increasing and therefore we are looking at regions of decreasing turbulent energy. But the largest measured admittances and distortions occur at the low frequency end of the spectrum, where it is fairly flat. A more useful limit may therefore be obtained by examining the zero-frequency intercept of the admittance in large-scale turbulence.

$$P_0(k_1 = 0) = (2C_D \sin k_2)/k_2,$$

as in (i); therefore

$$X_j(k_1 = 0) = 2C_D\left\{1 + \left(\frac{2\alpha}{\pi}\mathscr{M}\int_0^\infty F_j(\lambda)\,d\lambda\right)\Big/ L_1 + O(L_1^{-2})\right\} \quad \text{as} \quad L_1 \to \infty, \tag{20}$$

where $$\alpha = \pi^{\frac{1}{2}}\Gamma(\tfrac{5}{6})/\Gamma(\tfrac{1}{3}) \quad \text{and} \quad \mathscr{M} = 4K/(4+K)$$

is the mean source-like effect of the plate on the free stream due to the steady drag. The $O(1/L_1)$ term in (20) represents additional unsteady drag due to distortion of the oncoming turbulence. The admittance at zero frequency $A(0)$ is obtained by dividing (19) by $64s^2L_1C_D^2\overline{u}_{1\infty}^2$ and putting $\gamma = \sigma$. Integrating $F_j(\lambda)$ gives

$$A(0) = 1 + 0{\cdot}29\mathscr{M}L_1^{-1} + O(L_1^{-2}).$$

This predicts an $O(L_1^{-1})$ increase in $A(0)$ owing to distortion above the zero-frequency, infinite length scale value of 1. In the absence of distortion, Vickery's admittance (see Roberts 1971) can be expanded for large length scale as

$$A_v(0) = 1 - CL_1^{-2}.$$

(C is a positive constant.) This second term represents a reduction of the admittance owing to reduced coherence of the incident turbulence over the face of the plate as the characteristic eddy size gets smaller. The first-order distortion term is therefore of lower order than the second-order coherence effect, but in practice, because the constant C is numerically quite large, the coherence term dominates the distortion term at all length scales for which the latter is not negligible. A more useful asymptotic approximation for the effect of distortion is therefore

$$A(0) = A_v(0)\{1 + 0{\cdot}29\mathscr{M}L_1^{-1}\}.$$

Figure 6 shows this to give good agreement with the computed admittances at the low frequency end of the spectrum, even down to quite small length scales.

(iv) *Small length scales* ($L_1 \to 0$). The assumptions of rapid-distortion theory, and of the present linearized analysis make application of the theory doubtful in this case. Nevertheless, it is interesting to compare the asymptotic result obtained in this limit with the results of other methods. Hunt (1973) and Bearman (1971) both showed that, for sufficiently small length scales, the turbulence convected along the centre-line (stagnation streamline in their cases) undergoes a homogeneous plane strain. The velocity spectra at distances greater than $O(L_1)$ from the body can therefore be calculated from the formulae given by Batchelor & Proudman (1954). Figure 9 shows curves of the total streamwise intensity

$$\overline{u}^2 = \overline{(u_{1\infty} + u_1)^2}$$

calculated for zero length scale turbulence along the centre-line for various plates. The results of 'exact' homogeneous strain theory, and of the present linearized theory, are seen to agree, as should be expected, in regions where the flow perturbation is small (e.g. $< 10\%$ difference if $|\overline{u}_1| < 33\%$). The distortion function $F_j(\lambda)$ takes the same asymptotic form in the limit $L_1 \to 0$ as it did in case (ii) of high frequency. That is,

$$F_j(0) = \left\{\left(\tfrac{1}{2} - \frac{k_2^2 - k_1^2}{k^2}\right)\left(\delta_{1j} - \frac{k_1k_j}{k^2}\right) - \epsilon_{3jq}\frac{k_2k_q}{k^2}\right\}\exp\left[(\lambda - ik_1)x_1\right].$$

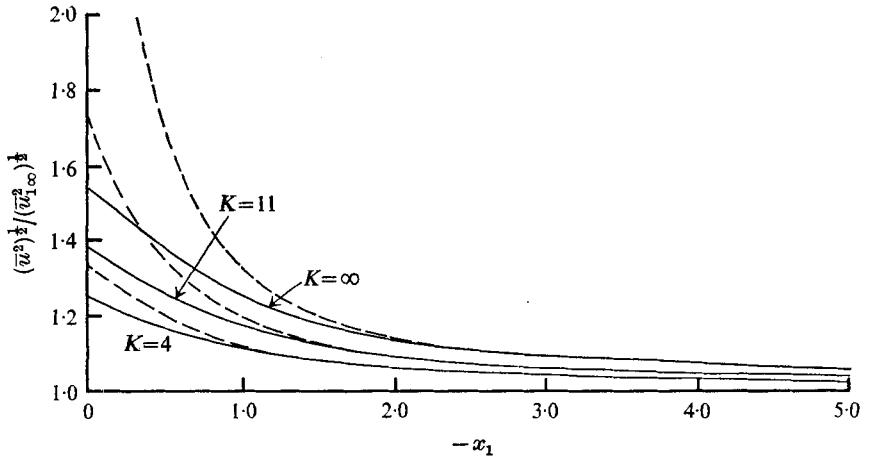

FIGURE 9. Asymptotic calculations of turbulence intensity on the centre-line, for $L_1 \to 0$. ——, linearized theory. – – –, homogeneous plane strain (Batchelor & Proudman 1954).

The irrotational (blockage) part $\partial\phi_1/\partial x_1$ of the velocity field is negligible provided $L_1/x_1 \to 0$. Substituting these into (19) gives the velocity spectrum

$$S'_{11}(k_1) = S_{11}(k_1)\left[1 + 2(1-\overline{\mathscr{U}}_1)\left\{1 - \tfrac{55}{12}k_1^2(\alpha^2+k_1^2)^{\frac{5}{6}}\int_0^\infty \frac{\tau d\tau}{(k_1^2+\tau)(\alpha^2+k_1^2+\tau)^{\frac{17}{6}}}\right\}\right].$$

The total streamwise intensity $\overline{u}^2$ is obtained by integrating (19) spherically over all wavenumbers, to give

$$\overline{u}^2 = \{1 + \tfrac{4}{5}(1-\overline{\mathscr{U}}_1) + \tfrac{43}{70}(1-\overline{\mathscr{U}}_1)^2\}\overline{u}_{1\infty}^2.$$

This may be compared with an expansion of the Batchelor & Proudman formula, for a small homogeneous plane strain (see e.g. Townsend 1954), as

$$\overline{u}^2 = \{1 + \tfrac{4}{5}(1-\overline{\mathscr{U}}_1) + \tfrac{26}{35}(1-\overline{\mathscr{U}}_1)^2 + O(1-\overline{\mathscr{U}}_1)^3\}\overline{u}_{1\infty}^2.$$

The two formulae agree to first order. The difference in the higher-order terms reflects the higher-order terms omitted from the turbulent vorticity transport equation in the linearized analysis presented here. In the extreme case of flow up to a stagnation point with $L_1 \to 0$, the linearized theory predicts a limiting value of $\overline{u}^2 = 2{\cdot}41\overline{u}_{1\infty}^2$ compared with the infinite intensity predicted by full rapid-distortion theory. Corresponding asymptotes for three-dimensional plates involve a smaller distortion; since they are more difficult to obtain, they have not been derived.

4.4. *Application to solid plates*

In view of the large amount of experimental data available for solid square plates, it seems worth while to attempt a comparison of predictions of the present method with solid plate data. In figure 5, computed values for a square isolated porous plate with $K = 4$ (the largest permissible value) are compared with Robert's (1971) theory based on the Vickery drag formula, and with some measured results, from a solid plate obtained by Bearman (1969) and from the present experiments. This shows that the correction for turbulence distortion given by the present calculation (at the small k_1 end of the spectrum) is of the right sense

and about half the required magnitude. In addition, the correction (see figure 6) acts so as to bring all the admittance spectra closer together for different L_1, an effect which is apparent in the experimental data. The asymptotic distortion analysis of (iii) for small k_1 and large L_1, is only applicable to two-dimensional solid plates. With this,

$$X_j = 2C_D\left[\delta_{ij} + \frac{2}{\pi}\mathscr{M}\alpha L_1^{-1}\int_0^\infty F_j(\lambda)\,d\lambda + O\{L_1^{-2}, k_1\}\right], \tag{21}$$

where $\alpha = \pi^{\frac{1}{2}}\Gamma(\frac{5}{6})/\Gamma(\frac{1}{3})$, $\mathscr{M}$ represents the total source effect due to the drag of the plate, and C_D in (21) should be given the experimentally determined value of mean drag coefficient for the plate. Thus, $C_D \simeq 1{\cdot}85$. The total source effect $\mathscr{M}$ could be related to the drag of the body, $\mathscr{M} = C_D$. But, in the case of high Reynolds number separated flows, it is more realistic to relate it to the width of the near wake. For a flat two-dimensional plate, the near-wake flow model of Parkinson & Jandali (1970) gives $\mathscr{M} = 4{\cdot}36$ for a base pressure coefficient $C_{pb} = -1{\cdot}08$. This is rather more than twice that given by $\mathscr{M} = C_D$. The limiting case of Taylor's theory with $K = \infty$ gives a similar value $\mathscr{M} = 4$. But the simplest general formula for bluff bodies is obtained from Maskell's (1963) wind tunnel blockage analysis, from which $\mathscr{M} = -2C_D/C_{pb} \simeq 3{\cdot}44$.

This last formula has been used to calculate the asymptotic admittance value given by § 4.3 for small k_1 and L_1^{-1}. The resulting value for a solid two-dimensional plate is shown in figure 5. Also included in this figure is the similar asymptotic result for $K = 20$ using the Taylor source value $4K/(4+K)$. By integrating $F_j(\lambda)$ in (21) as before, for a von Kármán spectrum, the admittance for low frequency components of the drag of a solid plate is

$$A(n) = A_0(n)\{1 - 0{\cdot}58C_D/C_{pb}L_1^{-1} + O(L_1^{-2})\}.$$

The relative success of this formula at moderate turbulence scales may be explained by the fact that much of the incident turbulent vorticity effecting the drag misses the region of intense strain close to the stagnation streamline. For this reason a similar analysis for the distorted velocity spectrum on the centreline would be less likely to be accurate. An admittance has similarly been calculated for the square solid plate and is shown in figure 5, in order to compare it with the experimental data.

The extension of Taylor's theory to $K = \infty$ does give tolerable agreement with solid plate data and with more accurate flow models (see figure 3), if the front face pressures are calculated from Bernoulli's theorem rather than from the resistance formula. But the extension of any such methods to unsteady flow is very difficult and there is also insufficient detailed experimental evidence to construct a model. In addition all such theories are really limited to predictions of front face pressures. Vickery's formula effectively rests on the assumptions that for a solid flat plate both the front face *and the base* pressures depend on some integrated value of the turbulent velocities in the neighbourhood of the plate and its near wake. Vickery chooses the unweighted integral of the normal velocities over the front face of the plate as the simplest representation of this integral, and this is probably a reasonable assumption in the quasi-steady case.

Appendix A. The solution of the equations for the potential

We define the *complete* Fourier transforms

$$\Phi = (2\pi)^{-\frac{3}{2}} \iiint_{-\infty}^{\infty} \phi \exp\left[i(\mu x_2 + \nu x_3 - \omega t)\right] dx_2 dx_3 dt,$$

and the *partial* transforms

$$\Phi_+ = (2\pi)^{-\frac{3}{2}} \iint_{-\infty}^{\infty} \int_{-b}^{b} \phi \exp\left[i(\mu x_2 + \nu x_3 - \omega t)\right] dx_2 dx_3 dt$$

with Φ_- correspondingly defined such that $\Phi = \Phi_+ + \Phi_-$. Thus e.g. Φ_+ is the transform of a function which is only non-zero for $|x_2| < 1$. Substitution of these transforms into $\nabla^2 \phi_i = 0$, with the condition that the appropriate ϕ_i is bounded in each half-space on either side of $x_1 = 0$ implies that the transform of $\partial\phi_1/\partial x_1$ is $\tau\Phi_1$ and of $\partial\phi_2/\partial x_1$ is $-\tau\Phi_2$, where $\tau = (\mu^2 + \nu^2)^{\frac{1}{2}}$, the positive root being taken. The transforms of (9) and (10) are

$$ik_1(\Phi_1 - \Phi_2) + \beta\tau(\Phi_1 + \Phi_2) = -\tfrac{1}{2}K\beta(U_+ + (\tau\Phi_1)_+),$$

and

$$ik_1\tau(\Phi_1 + \Phi_2) + \beta\tau^2(\Phi_1 - \Phi_2) = 0.$$

U_+ is the appropriate partial transform of u_1''. Eliminating Φ_2 gives

$$2(ik_1 + \beta\tau)\,\Phi_1 = -\tfrac{1}{2}K\beta(U_+ + (\tau\Phi_1)_+). \tag{A 1}$$

This type of problem can be solved by either an approximate application of the Wiener–Hopf technique or by use of Mellin transforms. However, the following alternative approach is convenient here. We write

$$-4(ik_1 + \beta\tau)\,\Phi_1 = P = P_+,$$

by the right-hand side of (A 1). P is actually the transform of Δp, the non-dimensional load distribution on the plate. Since $P = P_+$ and is proportional to U_1'', this transform can be expressed as a Neumann series

$$P = (2/\pi)\,\mu^{-1} \sum_{n=0}^{\infty} A_n J_{n+1}(\mu)\, U_1'',$$

where J_n is a Bessel function. (See e.g. Titchmarsh 1937, equation 11.22.) Substituting this into (A 1) gives, after some rearrangement,

$$\left(\frac{2}{\pi}\right)^{\frac{1}{2}} \mu^{-1} \left\{1 + \frac{K\beta\tau}{4(ik_1 + \beta\tau)}\right\} \sum_{n=0}^{\infty} A_n J_{n+1}(\mu) = K\beta(U_+ - (\tau\Phi_1)_-)/U_1'', \tag{A 2}$$

which completely specifies the problem. If (A 2) is multiplied by a set of + transforms $\Theta_{m+}(\mu)$ say, and then integrated with respect to μ between + and $-\infty$ the $(\tau\Phi_1)_-$ term drops out, since θ_m is zero wherever $\partial\phi_1/\partial x_1$ is non-zero.

A suitable set of functions for Θ_m is

$$\Theta_m = \mu^{-1} J_{m+1}(\mu), \quad m \geqslant 0.$$

Using these, and the result that

$$\int_{-\infty}^{\infty} U_+ \Theta_{m+}(\mu)\, d\mu = (2\pi)^{\frac{1}{2}}\, U_1' \Theta_{m+}(-k_2),$$

the set of linear equations obtained can be truncated by assuming P_n negligible for $n \geqslant N$, and solved as separated sets of even and odd equations:

$$\sum_{n=1}^{N} P_{n-1}\left\{\int_0^\infty \mu^{-2} J_n(\mu)\, J_m(\mu)\left(1+\frac{K\beta\tau}{4(ik_1+\beta\tau)}\right)d\mu\right\} = \frac{\pi}{2}\frac{K\beta}{k_2} J_m(k_2), \quad m = 1, \ldots, N. \tag{A 3}$$

The summation is over odd values when m is odd, and even when m is even. The coefficients A_n correspond to weighted moments of the load distribution Δp. Thus e.g.

$$P_{2m} = (-1)^m (4m+2) \sum_{n=0}^{m}{}' \int_{-1}^{1} T_{2n}(x_2)\, \Delta p\, dx_2 / U_1''.$$

T_n is a Chebyshev polynomial. In particular, the sectional drag of the plate is

$$D = P_0 U_1'' \exp\left[i(\omega t - k_3 x_3)\right].$$

Similarly the velocity component $\partial\phi_1/\partial x_1$ on the centre-line upstream of the plate is given by

$$\left.\frac{\partial\phi_1}{\partial x_1}\right|_{x_2=0} = -\frac{U_1'' \exp\left[i(\omega t - k_3 x_3)\right]}{2\pi} \sum_{n=0}^{\frac{1}{2}N} P_{2n} \int_0^\infty \left(J_{2n+1}(\mu)\, \tau \exp(\tau x_1)/(ik_1\mu + \beta\mu\tau)\right) d\mu.$$

The non-tabulated parts of the integrals in (A 3) were integrated numerically.

Appendix B. Calculation of U' from the distorted turbulent vorticity field

The Biot–Savart contribution to (2) can be written, in an abbreviated notation,

$$u_i' = u_{i\infty} + \mathscr{L}_{ij}\{g_{jp}(\mathbf{x}, \bar{\mathbf{u}})\}\, \mathrm{Z}_{p\infty} \exp\left[i(\omega t - k_3 x_3)\right].$$

$\mathscr{L}_{ij}$ is a linear matrix operator (the Biot–Savart integral); and g_{jp} is a linear function of the mean disturbance velocity. This linearity, which followed from the smallness of $|\bar{\mathbf{u}}|$ in the main regions of contribution to $\mathscr{L}$, is essential to the following analysis.

Suppose

$$g_{jp} = g_{jp}(\mathbf{x}, \bar{\mathbf{u}}, y),$$

when $\bar{\mathbf{u}}$ is the mean disturbance velocity of a unit density line source placed at $(x_1 = 0, x_2 = y)$ in the stream. Then, in the case of the porous plate,

$$u_j' = u_{i\infty} + \mathscr{L}_{ij}\left\{\int_{-\infty}^{\infty} m(y)\, g_{jp}(y)\, dy\right\} \mathrm{Z}_{p\infty} \exp\left[i(\omega t - k_3 x_3)\right]$$

where

$$m(y) = \begin{cases} 0, & |y| > 1, \\ 2K/(4+K), & |y| < 1, \end{cases}$$

is the source distribution representing the plate. Therefore, taking the negative Fourier transform $M(-\lambda)$ of $m(y)$, where

$$M(-\lambda) = \frac{4K}{4+K}\frac{\sin\lambda}{\pi\lambda},$$

gives

$$u_i' = u_{i\infty} + \left\{\int_0^\infty \frac{\sin\lambda}{\pi\lambda}\, \mathscr{L}_{ij}(G_{jp}(\lambda))\, d\lambda\right\} \mathrm{Z}_{p\infty} \exp\left[i(\omega t - k_3 x_3)\right]. \tag{B 1}$$

$G(\lambda)$ is the transform of $g(y)$. The order of integration is assumed to be interchangeable, and the identity

$$\int_{-\infty}^{\infty} m(y)\, g(y)\, dy = \int_{-\infty}^{\infty} M(-\lambda)\, G(\lambda)\, d\lambda$$

has been used. The reason for this manoeuvre is that $\mathscr{L}_{ij}(G)$ can be integrated analytically, whereas $\mathscr{L}_{ij}\left\{\int_{-\infty}^{\infty} mg(y)\, dy\right\}$ (i.e. direct evaluation from the velocity field of the plate) apparently cannot.

Therefore, since

$$\boldsymbol{\zeta}_\infty = -i\mathbf{k}\times\mathbf{U}\exp[i(\omega t-\mathbf{k}.\mathbf{x})],$$

$$u_1' = U_{j\infty}\exp[i(\omega t-k_3x_3)]\left\{\exp[-i(k_1x_1+k_2x_2)]\delta_{ij}+\frac{4K}{4+K}\int_0^\infty \frac{\sin\lambda}{\pi\lambda}F_j(\lambda,\mathbf{x})\,d\lambda\right\}. \tag{B 2}$$

F can be expressed as an algebraic expression in λ and k by carrying out the Biot–Savart integration $\mathscr{L}_{ij}$ on the Fourier components $G_{jp}(\lambda)$ of the mean disturbance velocity:

$$\begin{aligned}
F_j(\lambda,\mathbf{x}) = \frac{1}{4}\sum_{n=1}^{2}\Bigg\{&\frac{(-1)^n k_q}{\lambda}\Bigg[\left(\frac{(-1)^n ik_1}{k_q}\left(\delta_{1j}-\frac{k_1k_j}{k^2}\right)\right.\\
&\left.+\frac{i\lambda k_3\epsilon_{1jq}+ik_3((-1)^n k_1+i\alpha_{3-n})\epsilon_{2jq}+\alpha_n(k_2-i(-1)^n k_1\epsilon_{3jq})}{(\beta_n^2-(\lambda-ik_1)^2)}\right)\\
&\times\exp[\lambda x_1-i(k_1x_1+k_2x_2)]\\
&+\left(\frac{ik_1\lambda}{\gamma_n^2}(k_3\epsilon_{2jq}-\alpha_n\epsilon_{3jq})(-1)^n+\frac{\alpha_nk_2\epsilon_{3jq}-\alpha_{3-n}k_3\epsilon_{2jq}}{\gamma_n}\right.\\
&\left.+\frac{ik_3\lambda^2\epsilon_{1jq}-ik_3(k_1k_2-i\alpha_{3-n}\beta_n)\epsilon_{2jq}+\alpha_n(ik_1\alpha_n+k_2\beta_n)\epsilon_{3jq}}{\lambda^2-\gamma_n^2}\right)\\
&\times\exp[\beta_nx_1-i\alpha_nx_2]\Bigg]\Bigg\},
\end{aligned}$$

where

$$k^2 = k_1^2+k_2^2+k_3^2,\quad \alpha_n = k_2-(-1)^n\lambda,\quad \beta_n = (\alpha_n^2+k_3^2)^{\frac{1}{2}}\quad\text{and}\quad \gamma_n = \beta_n+ik_1.$$

The final integration with respect to λ in (B 2) was carried out numerically.

REFERENCES

Batchelor, G. K. & Proudman, I. 1954 *Quart. J. Mech. Appl. Math.* **7**, 83.

Bearman, P. W. 1969 *Nat. Phys. Lab. Aero. Rep.* no. 1296.

Bearman, P. W. 1971 *J. Fluid Mech.* **53**, 451.

Blockley, R. H. 1968 M.Sc. thesis. Department of Aeronautics, London University.

Castro, I. P. 1971 *J. Fluid Mech.* **46**, 599.

Darwin, C. G. 1953 *Proc. Camb. Phil. Soc.* **49**, 342.

Davenport, A. G. 1961 *Proc. Inst. Civ. Engrs*, **19**, 449.

DeBray, B. G. 1957 *Aero. Res. Counc. CP* 343.

Elder, J. W. 1959 *J. Fluid Mech.* **5**, 355.

Graham, J. M. R. 1972 *Imperial College, Aero. Rep.* no. 72–20.

HARRIS, R. I. 1970 *CIRIA Seminar on Wind-Sensitive Structures, Inst. Civ. Engrs*, paper 3.

HUNT, J. C. R. 1972 *IUTAM/IAHR Symp. on Flow-Induced Structural Vibrations, Karlsruhe*, paper B 5.

HUNT, J. C. R. 1973 *J. Fluid Mech.* **61**, 625.

KOO, J.-K. & JAMES, D. F. 1973 *J. Fluid Mech.* **60**, 513.

LAU, Y. L. & BAINES, W. D. 1968 *J. Fluid Mech.* **33**, 721.

LIGHTHILL, M. J. 1956 *J. Fluid Mech.* **1**, 31.

MASKELL, E. C. 1963 *Royal Aircraft Est. Aero. Rep.* no. 2685.

OWEN, P. R. & ZIENKIEWICZ, K. H. 1957 *J. Fluid Mech.* **2**, 521.

PARKINSON, G. V. & JANDALI, T. 1970 *J. Fluid Mech.* **40**, 577.

RIBNER, H. S. & TUCKER, M. 1952 *Nat. Adv. Com. Aero. Tech. Note*, no. 2606.

ROBERTS, J. B. 1971 *Nat. Phys. Lab. Aero. Rep.* no. 1329.

SCHUBAUER, G. B., SPANGENBERG, W. G. & KLEBANOFF, P. S. 1950 *Nat. Adv. Com. Aero. Tech. Note* no. 2001.

TAYLOR, G. I. 1944 *Aero. Res. Counc. R. & M.* no. 2236.

TAYLOR, G. I. & BATCHELOR, G. K. 1949 *Quart. J. Mech. Appl. Math.* **2**, 1.

TAYLOR, G. I. & DAVIES, R. M. 1944 *Aero. Res. Counc. R. & M.* no. 2237.

TITCHMARSH, E. C. 1937 *Introduction to the Theory of Fourier Integrals*. Oxford University Press.

TOWNSEND, A. A. 1954 *Quart. J. Mech. Appl. Math.* **7**, 104.

TUCKER, H. J. & REYNOLDS, A. J. 1968 *J. Fluid Mech.* **32**, 657.

TURNER, J. T. 1969 *J. Fluid Mech.* **36**, 367.

VALENSI, J. & REBONT, J. 1969 *AGARD C.P.* 48, paper 27.

VICKERY, B. J. 1965 *Nat. Phys. Lab. Aero. Rep.* 1143.